Unizik Journal of Technology, Production and Mechanical Systems (UJTPMS)

journal homepage: https://journals.unizik.edu.ng/index.php/ujtpms/about
PRINT ISSN: 1115-7143 || ONLINE ISSN: 1115-7453

Temperature-Driven Dynamics of Small Spherical Particle Adhesion on Submerged Substrates: Mechanisms and Interfacial Interactions

Okwuchukwu Innocent Ani [1*]; Thomas Chinedu Aniokete[2]; Alfred Ogbodo Agbo[3].

[1]Department of Mechanical and Production, Enugu State University of Science and Technology, Agbani, Enugu, Enugu State.
[2] Department of Chemical Engineering, Enugu State University of Science and Technology, Agbani, Enugu, Enugu State.
[3] Department of Materials and Metallurgical Engineering, Enugu State University of Science and Technology, Agbani, Enugu, Enugu State.

ARTICLE INFO

Article history:
Received March. 2, 2025
Revised March 20, 2025
Accepted April 14, 2025

Available online April 17, 2025

Keywords:
Particle adhesion mechanisms, Temperature-dependent interfacial forces, Submerged substrate interactions, van der Waals and Electrostatic forces, Hamaker coefficient analysis

ABSTRACT

Understanding the adhesion dynamics of small spherical particles on submerged substrates is crucial for various applications in colloidal science, materials engineering, and industrial processes. This study investigates the force required to initiate the rolling motion of glass spheres on an inclined glass surface in water and ethanol, examining the effect of temperature on this force. The results confirm the presence of van der Waals attractions between the spheres and the substrate, which are weakened by thermal energy. As temperature increased, the liquid matrices expanded, reducing density while decreasing the angle of inclination needed for particle motion. This reduction was attributed to a decrease in the coefficient of friction with rising temperature. The Hamaker coefficient, derived from the experimental data, ranged from 1.986×10^{-15} to 5.296×10^{-15} mJ/m² in water and 2.262×10^{-15} to 5.278×10^{-15} mJ/m² in ethanol, suggest agreement with literature values and showing a tendency to increase with temperature. Similarly, the coefficient of friction decreased from 0.0680 to 0.0400 in water and from 0.0480 to 0.0326 in ethanol, further supports the role of thermal energy in modifying interfacial interactions. These findings provide insights into the thermally driven adhesion mechanisms of submerged particles, with implications for optimizing material handling, coating technologies, and microfluidic systems.

1. Introduction

The adhesion of small spherical particles to solid substrates immersed in liquids is a phenomenon of significant importance across various scientific and industrial domains, including colloidal science, materials engineering, and surface chemistry. This adhesion is predominantly governed by intermolecular forces, notably van der Waals and electrostatic interactions. Understanding how these forces are influenced by environmental factors, such as temperature, is pivotal for optimizing processes like coating technologies, material handling, and microfluidic system design. Van der Waals forces are weak intermolecular attractions that arise from transient dipole moments in atoms or molecules, leading to interactions between particles and substrates, playing a pivotal role in the stability and behavior of colloidal systems between electrically neutral entities. These forces are inherently short-range and diminish rapidly as the distance between interacting particles increases [1; 2]. In the context of particle adhesion, van der Waals forces facilitate the attraction

Electrostatic forces, on the other hand, result from the presence of surface charges on particles and substrates. These forces can be either attractive or repulsive, depending on the nature of the charges involved. In liquid media, the distribution of ions can shield these charges, affecting the net electrostatic interaction. The balance between van der Waals and electrostatic forces

*Corresponding author: okwuchukwu.ani@esut.edu.ng

determines whether particles adhere to or disperse from a substrate [3]. Temperature is a critical factor influencing these intermolecular forces. As temperature increases, thermal agitation can disrupt the attractive interactions between particles and substrates, potentially weakening adhesion. This thermal energy can alter the dielectric properties of the medium, subsequently affecting the magnitude of van der Waals forces. For instance, the Hamaker constant, which quantifies the strength of van der Waals interactions, has been shown to vary with temperature due to changes in the dielectric constant and refractive index of the medium [4; 5]. Additionally, elevated temperatures can influence electrostatic interactions by modifying ion distribution and mobility within the liquid, thereby affecting the Debye length and the extent of electrostatic screening [4; 6].

The Hamaker constant (A132) plays a key role in understanding van der Waals interactions in systems where two materials are separated by a medium. Its value determines whether the interaction is attractive or repulsive; when positive, the materials attract each other, and when negative, they repel [7; 8]. For a spherical particle with radius R suspended in a liquid and positioned a short distance d from a solid surface, the van der Waals force (F) can be estimated using the Hamaker relation. This equation shows that the force is directly proportional to both the Hamaker constant and the particle's radius. In simple terms, larger particles experience stronger van der Waals forces. However, the force is inversely proportional to the square of the separation distance, meaning it weakens quickly as the gap between the particle and the surface increases. Temperature also affects the Hamaker constant, which means that changes in temperature can influence how strongly particles adhere to surfaces. This is important in many fields, including nanotechnology, materials science, and biomedical engineering, where controlling adhesion and stability is crucial [8].

Several experimental techniques have been developed to measure adhesion forces between particles and planar surfaces. The inclined plane method is particularly effective for larger spherical particles (greater than 2 μm in diameter) [9; 10]. In this method, particles are placed on an inclined surface, and the angle at which they begin to roll or slide is recorded. This critical angle correlates with the adhesive forces at play. Other methods include centrifuge techniques, which are suitable for submicron particles, and aerodynamic or hydrodynamic approaches that assess particle detachment under fluid flow conditions [11; 12]. Understanding the interplay between particle adhesion and temperature has both theoretical and practical implications. For instance, in processes involving high temperatures, such as material fabrication or thermal treatments, controlling particle adhesion is essential to ensure product quality and process efficiency [13]. Studies have shown that as temperature increases, the adhesive forces between particles and substrates can decrease, facilitating easier particle removal or redistribution [14; 15; 16]. This temperature-dependent behavior is crucial for applications like preventing fouling in heat exchangers or optimizing particle deposition in coating processes [17].

Understanding these interactions aids in controlling the microstructure and properties of composite materials [18; 19; 20]. The adhesion of small spherical particles to substrates immersed in liquids is a complex phenomenon influenced by van der Waals and electrostatic forces. Temperature plays a pivotal role in modulating these interactions by altering the physical properties of the medium and the interacting bodies. A comprehensive understanding of these mechanisms is essential for optimizing various industrial and scientific applications, from material synthesis to surface treatment processes [21]. The adhesion of small spherical particles to solid substrates immersed in liquids has been a subject of extensive research due to its significance in various industrial and scientific applications, including material processing, coatings, and colloidal stability. Early studies, such as those by [22], investigated the fundamental mechanisms of adhesion, identifying capillary forces, intermolecular interactions, and coalescence by dissolution as primary contributors. However, his research did not provide clarity on the role of electrostatic charge, suggesting that electrostatic attraction after contact contributes minimally to adhesion mechanisms. [14] expanded on this knowledge by examining the adhesion of atmospheric dust particles to solid surfaces. Their research revealed the persistence of dust adhesion and emphasized the importance of particle and substrate properties as well as ambient environmental conditions. Their findings spurred further research into adhesion forces, laying the groundwork for more quantitative studies on small particle adhesion. [23] explored the humidity dependency of small particle adhesion, focusing on silica and titania surfaces. Their experiments demonstrated that humidity influences adhesion through capillary bridge formation, particularly affecting micro and sub-micro particles. Their results underscored the role of surface roughness and particle shape in adhesion behavior, providing critical insights into humidity-driven adhesion mechanisms. Building on these findings, [20] specifically investigated the adhesion of small spherical particles to substrates immersed in liquids. They examined van der Waals attractions and determined the Hamaker coefficients for different liquid systems, highlighting the importance of intermolecular forces in adhesion.

More recent studies, such as those by [24], have delved into substrate morphology and chemical interactions affecting adhesion. Copper et al. demonstrated that surface roughness and chemical reactions can dynamically alter adhesion properties, while Beaudoin et al. developed models incorporating electrostatic, van der Waals, and hydrophobic interactions, which have applications in semiconductor cleaning, biomaterials, and detection technologies. Despite these advancements, the influence of temperature on particle adhesion in liquid media remains underexplored. This study aims to bridge this gap by determining the effect of temperature on adhesion in liquid environments like water and ethanol

2. Materials and Methods

2.1. Materials and Sample Preparation

Small silica spherical particles of known size distribution were selected. Solid substrates such as copper-coated glass and silicon wafers were cleaned and prepared. Liquid media (water and ethanol) were used to immerse the samples under controlled conditions.b

2.2. Experimental Setup

An inclined plane apparatus was used to measure adhesion forces by monitoring particle motion under different temperatures. Temperature-controlled chambers were employed to maintain precise environmental conditions. High-resolution optical microscopy and atomic force microscopy (AFM) were used to observe adhesion behavior at the microscale.

2.3. Measurement of Adhesion Forces

The critical force required for rolling or detaching the particles was determined using the inclined plane method. Centrifuge and hydrodynamic techniques were applied for comparative adhesion force measurements. The Hamaker coefficient was estimated based on experimental data and theoretical models.

2.4. Effect of Temperature Variation

Experiments were conducted at multiple temperature points (e.g., 20°C, 40°C, 60°C, 80°C) to study thermal effects on adhesion. Data on particle-substrate interaction at different temperatures were recorded and analyzed.

2.5. Data Analysis and Theoretical Modeling

Statistical analysis was performed to determine the significance of temperature effects. Theoretical adhesion models were refined based on experimental findings while results are compared with existing literature to validate the study's findings in the following sections.

2.6. Calculation of Hamaker Coefficients.

The Hamaker constant (A_{132}) is a fundamental parameter in quantifying van der Waals interactions in a system comprising two materials (***1*** and ***2***) separated by a medium (***3***). When $\boldsymbol{A_{132}}$ is positive, the interaction is attractive; when negative, it is repulsive. For a spherical particle of radius ***R*** suspended in a liquid at temperature ***T*** and separated from a planar solid substrate by a distance ***d***, the van der Waals force F, can be approximated using the Hamaker relation [7; 8].

$$F = \frac{A_{132}}{6d^2} R \ , \tag{1}$$

demonstrating that the van der Waals force is directly proportional to the Hamaker constant and the particle's radius, and inversely proportional to the square of the separating distance, ***d***. As temperature affects the Hamaker constant, it consequently influences the magnitude of the adhesion force between particles and substrates.

The straight lines drawn on the graphs plotted in Figure 5 and Figure 6, were obtained by linear regression. This positive slope of these lines demonstrate van der Waals forces are attractive and the particles will touch the solid substrate. This justifies the use of $\mathbf{d_o}$, the minimal distance between the particle and the substrate, instead of the variable distance **d**, used in equation above. Using $\mathbf{d_o}$ = 2A, we calculated the friction coefficients and the Hamaker coefficients of two systems: friction coefficients are obtained from the intercept of the straight lines with the vertical axis, and Hamaker coefficients from the slope B of the straight lines by using the relation:

$$A_{132} = \frac{B8\pi d_o^{\ 2}(\rho_1 - \rho_2)g}{\mu} \tag{2}$$

Where μ is calculated from equation 2

$$A = \mu \cos\phi \tag{3}$$

and $$B = \mu \frac{A_{132}}{6d^2 \frac{4\pi}{3}(\rho_1 - \rho_2)g} \tag{4}$$

and taking the density of glass spheres as ρ_1 = 2.5g/ml = 2.5g/cm^3 or 2500kg/m^3, and that of Ethanol at 20^{o}C as ρ_2 = 0.7893g/cm^3 or 789.3kg/m^3.

3. Results and Discussion

The first experiment was conducted with water at room temperature $(27^oC \pm 2)$ and subsequently with Ethanol at room temperature.

3.1. Water at Room Temperature

Table 1: Angles for which rolling occurs for water as test liquid for Glass spheres at Room Temperature**.**

Particle Diameter D(cm)	**L(cm)**	**h(cm)**	**1/R^2 (cm^{-2})**	**sin Ø = $^h/_L$**
0.4500	3	0.27	19.75	0.0910
0.4500	4	0.38	19.75	0.0940
0.4500	5	0.45	19.75	0.0905
0.0190	3	0.55	110.80	0.1844
0.0165	3	0.59	146.92	0.1927

0.0155	3	0.81	16649.26	0.2692
0.0150	3	0.73	17776.89	0.2449
0.0135	3	0.82	21942.00	0.2743

The angles of inclination at which sliding or rolling of the glass spheres occurred in water and in Ethanol at room temperature are listed in Tables 1 and 2 respectively. In the two cases, the general trend is an increase of the angle of inclination at which rolling occurs, with decreasing particle size. The density of pure water (0.9982g/cm^3 or 998.2kg/cm^3) is greater than that of Ethanol (0.7893g/cm^3 or 789.3kg/cm^3) at same temperature 20^{O}C. The angle of inclination was smaller in Ethanol than in water for the same type of particles [25]. That is, a given particle commences sliding earlier as angle of inclination is increased in a less dense liquid. The larger the particles, the faster they will slide along the glass slide, hence the smaller the vertical height measured. This shows that apparent weight of particles affects their adhesion to substrates. It is interesting to plot our results in the form $\sin\phi = f(\frac{1}{R^2})$, this means that $\sin\phi$ is a function of inverse of the square of the radius of the particles. The constants A and B denote intercept on y-axis and the slope of the graph of $\sin\phi$ against $1/R^2$. The graphs for water and Ethanol systems have been plotted. Each point represents an average of several values.

Table 2: Angles for which Rolling occurs with Ethanol as the test liquid for glass spheres at room Temperature.

Particle Diameter D(cm)	**L(cm)**	**h(cm)**	**$1/R^2$ (cm^{-2})**	**sin Ø = $^h/_L$**
0.0190	3	0.39	11079.67	0.1300
0.0182	3	0.41	12075.84	0.1351
0.0170	3	0.47	13841.52	0.1582
0.0160	3	0.53	15625.00	0.1775
0.0150	3	0.53	17776.89	0.1772
0.0140	3	0.57	20408.98	0.1895

In spite of the scatter of the experimental results, the best fits for the experiment points are straight lines, which verifies the equation: $\sin\phi = A + \frac{B}{R^2}$ and validate the assumption that electrostatic effects were negligible in our systems. The straight lines drawn on the graphs plotted were obtained by linear regression. This positive slope of these lines shows van der Waals forces are attractive and the particles will touch the solid substrate. This justifies the use of $\mathbf{d_o}$, the minimal distance between the particle and the substrate, instead of the variable distance **d**, used in equation above.
Using $\mathbf{d_o}$ = 2A, we calculate the friction coefficients and the Hamaker coefficients of the two systems: friction coefficients are obtained from the intercept of the straight lines with the vertical axis, and Hamaker coefficients from the slope B of the straight lines by using the relation:

$$A_{132} = \frac{B8\pi d_o^{\,2}(\rho_1 - \rho_2)g}{\mu} \qquad (5)$$

and taking the density of glass spheres as ρ_1 = 2.5g/ml = 2.5g/cm^3 or 2500kg/m^3, and that of ethanol at 20^{o}C as ρ_2 = 0.7893g/cm^3 or 789.3kg/m^3. Values of the static friction coefficient μ , and the Hamaker coefficient A_{132} are given in Table 3 for the systems studied. All friction coefficients are between 0.0975 and 0.1650 which is quite reasonable

Table 3: Static friction coefficient μ, slope m of the straight line obtained by linear regression and Hamaker coefficient A_{132} for the systems studied.

S/N	**System**	**Friction Coefficient, μ**	**Slope M of the Straight line (cm^2)**	**Correlation Coefficient**	**Hamaker Coefficient A_{132} (mJ/m^2)**
1	Glass spheres on substrate in water (without heat)	0.1650	1.478×10^{-5}	0.98	1.324×10^{-15}
2	Glass spheres on substrate in water (with heat)	0.0975	8.73×10^{-6}	0.98	1.320×10^{-15}
3	Glass spheres on substrate in				

	Ethanol (without heat)	0.0800	7.16×10^{-6}	0.96	1.508×10^{-15}
4	Glass spheres on substrate in Ethanol (with heat)	0.0670	6.00×10^{-6}	0.94	1.500×10^{-15}

Hamaker Coefficients are between 1.320×10^{-15} and 1.508×10^{-15} mJ/m^2. They fall in the range of usual values for Hamaker Coefficients (between 10^{-15} and 10^{-13} mJ/m^2) and correspond to rather weak interactions. This indicates that there are van der Waals forces responsible for the adhesion of the small particles (glass spheres) in liquid matrix. For water, the experimental points for the larger glass spheres were and Hamaker plotted in Figures 1 and 2 also, and that led to a more accurate determination of the friction and Hamaker coefficients.

3.2. Water Matrix at Different Temperatures.

The experiment was repeated with glass particles deposited on the glass slide maintained at different temperatures ranging from 30ºC to 90ºC. The results are presented on Tables 4 – 9, and are summarized in Table 15.

Table 4: Angles for which rolling occurs for water as test liquid at different temperatures for glass sphere of Diameter 0.0427cm

Particle Diameter D(cm)	**Temp θºC**	**L(cm)**	**h(cm)**	**sin Ø = $^{h}/_{L}$**
0.0427	30	5	0.38	0.0760
0.0427	35	5	0.37	0.0740
0.0427	40	5	0.36	0.0720
0.0427	45	5	0.35	0.0700
0.0427	50	5	0.33	0.0660
0.0427	55	5	0.30	0.0600
0.0427	60	5	0.28	0.0560
0.0427	65	5	0.27	0.0540
0.0427	70	5	0.25	0.0500
0.0427	75	5	0.24	0.0480
0.0427	80	5	0.22	0.0440
0.0427	85	5	0.21	0.0420
0.0427	90	5	0.20	0.0400

Table 5: Angles for which rolling occurs for water as test liquid at Different Temperatures for glass spheres of Diameter 0.0395cm**.**

Particle Diameter D(cm)	**Temp θºC**	**L(cm)**	**h(cm)**	**sin Ø = $^{h}/_{L}$**
0.0395	30	5	0.43	0.0860
0.0395	35	5	0.42	0.0840
0.0395	40	5	0.40	0.0800
0.0395	45	5	0.37	0.0740
0.0395	50	5	0.36	0.0720
0.0395	55	5	0.35	0.0700
0.0395	60	5	0.33	0.0660
0.0395	65	5	0.32	0.0640
0.0395	70	5	0.30	0.0600
0.0395	75	5	0.29	0.0580
0.0395	80	5	0.27	0.0540
0.0395	85	5	0.25	0.0500
0.0395	90	5	0.24	0.0480

Table 6: Angles for which rolling occurs for water as test liquid at Different Temperatures from glass spheres of Diameter 0.0285cm

Particle Diameter D(cm)	**Temp θºC**	**L(cm)**	**h(cm)**	**sin Ø = $^{h}/_{L}$**
0.0285	30	5	0.40	0.0800
0.0285	35	5	0.39	0.0780
0.0285	40	5	0.38	0.0760
0.0285	45	5	0.36	0.0720
0.0285	50	5	0.35	0.0700
0.0285	55	5	0.35	0.0700

0.0285	60	5	0.33	0.0660
0.0285	65	5	0.32	0.0640
0.0285	70	5	0.30	0.0600
0.0285	75	5	0.29	0.0580
0.0285	80	5	0.27	0.0540
0.0285	85	5	0.26	0.0520

Table 7: Angles for which rolling occurs for water as test liquid at Different Temperatures from glass spheres of Diameter 0.0203cm

Particle Diameter D(cm)	**Temp θºC**	**L(cm)**	**h(cm)**	**sin Ø = $^{h}/_{L}$**
0.0203	30	5	0.49	0.0980
0.0203	35	5	0.48	0.0960
0.0203	40	5	0.46	0.0920
0.0203	45	5	0.45	0.0900
0.0203	50	5	0.43	0.0860
0.0203	55	5	0.39	0.0780
0.0203	60	5	0.38	0.0760
0.0203	65	5	0.37	0.0740
0.0203	70	5	0.36	0.0720
0.0203	75	5	0.34	0.0680
0.0203	80	5	0.32	0.0640
0.0203	85	5	0.31	0.0620

Table 8: Angles for which rolling occurs for water as test liquid at Different Temperatures form glass spheres of Diameter 0.0165cm**.**

Particle Diameter D(cm)	**Temp θºC**	**L(cm)**	**h(cm)**	**sin Ø = $^{h}/_{L}$**
0.0165	30	5	0.55	0.1100
0.0165	35	5	0.54	0.1080
0.0165	40	5	0.53	0.1060
0.0165	45	5	0.52	0.1040
0.0165	50	5	0.50	0.1000
0.0165	55	5	0.47	0.0940
0.0165	60	5	0.45	0.0900
0.0165	65	5	0.44	0.0880
0.0165	70	5	0.43	0.0860
0.0165	75	5	0.40	0.0800
0.0165	80	5	0.38	0.0760
0.0165	85	5	0.37	0.0740
0.0165	90	5	0.33	0.0660

Table 9: Angles for which rolling occurs for water as test liquid at Different Temperatures form glass spheres of Diameter 0.0107cm.

Particle Diameter D(cm)	**Temp θºC**	**L(cm)**	**h(cm)**	**sin Ø = $^{h}/_{L}$**
0.0107	30	5	0.78	0.1560
0.0107	35	5	0.74	0.1480
0.0107	40	5	0.68	0.1360
0.0107	45	5	0.64	0.1280
0.0107	50	5	0.59	0.1180
0.0107	55	5	0.57	0.1140
0.0107	60	5	0.55	0.1100
0.0107	65	5	0.46	0.0920
0.0107	70	5	0.42	0.0840

0.0107	75	5	0.40	0.0800
0.0107	80	5	0.39	0.0780
0.0107	85	5	0.37	0.0740
0.0107	90	5	0.36	0.0720

3.3. With Ethanol Matrix at Different Temperatures.

Using Ethanol as a test liquid, the angle at which the glass particles began rolling when immersed in Ethanol maintained at different temperatures ranging from 30ºC to 70ºC. The results are presented on Tables 10 – 14, and are summarized in Table 15.

Table 10: Angles for which rolling occurs for Ethanol as test liquid at different temperatures for glass sphere of Diameter 0.0427cm**.**

Particle Diameter D(cm)	Temp θºC	L(cm)	h(cm)	sin Ø = $^{h}/_{L}$
0.0427	30	5	0.50	0.1000
0.0427	35	5	0.48	0.0960
0.0427	40	5	0.47	0.0940
0.0427	45	5	0.43	0.0860
0.0427	50	5	0.41	0.0820
0.0427	55	5	0.40	0.0800
0.0427	60	5	0.37	0.0740
0.0427	65	5	0.34	0.0680
0.0427	70	5	0.31	0.0620

Table 11: Angles for which rolling occurs for Ethanol as test liquid at different temperatures for glass sphere of Diameter 0.0395cm**.**

Particle Diameter D(cm)	Temp θºC	L(cm)	h(cm)	sin Ø = $^{h}/_{L}$
0.0395	30	5	0.57	0.1140
0.0395	35	5	0.55	0.1100
0.0395	40	5	0.54	0.1080
0.0395	45	5	0.53	0.1060
0.0395	50	5	0.50	0.1000
0.0395	55	5	0.48	0.0960
0.0395	60	5	0.45	0.0900
0.0395	65	5	0.40	0.0800
0.0395	70	5	0.37	0.0740

Table 12: Angles for which rolling occurs for Ethanol as test liquid at different temperatures for glass sphere of Diameter 0.0285cm.

Particle Diameter D(cm)	Temp θºC	L(cm)	h(cm)	sin Ø = $^{h}/_{L}$
0.0285	30	5	0.60	0.1200
0.0285	35	5	0.59	0.1180
0.0285	40	5	0.56	0.1120
0.0285	45	5	0.55	0.1100
0.0285	50	5	0.53	0.1040
0.0285	55	5	0.49	0.0980
0.0285	60	5	0.47	0.0940
0.0285	65	5	0.43	0.0860
0.0285	70	5	0.39	0.0780

Table 13: Angles for which rolling occurs for Ethanol as test liquid at different temperatures for glass sphere of Diameter 0.0203cm.

Particle Diameter D(cm)	Temp θ°C	L(cm)	h(cm)	sin Ø = $^{h}/_{L}$
0.0203	30	5	0.66	0.1380
0.0203	35	5	0.64	0.1280
0.0203	40	5	0.63	0.1260
0.0203	45	5	0.63	0.1260
0.0203	50	5	0.61	0.1220
0.0203	55	5	0.58	0.1160
0.0203	60	5	0.57	0.1140
0.0203	65	5	0.52	0.1040
0.0203	70	5	0.48	0.0960

Table 14: Angles for which rolling occurs for Ethanol as test liquid at different temperatures for glass sphere of Diameter 0.0165cm**.**

Particle Diameter D(cm)	Temp θ°C	L(cm)	h(cm)	sin Ø = $^{h}/_{L}$
0.0165	30	5	0.75	0.1500
0.0165	35	5	0.73	0.1500
0.0165	40	5	0.70	0.1400
0.0165	45	5	0.64	0.1280
0.0165	50	5	0.62	0.1240
0.0165	55	5	0.58	0.1160
0.0165	60	5	0.55	0.1100
0.0165	65	5	0.53	0.1060
0.0165	70	5	0.51	0.1020

Table 15: Angle at which rolling occurs with Water as a test liquid at different temperatures.

Θ	30°C	40°C	50°C	60°C	70°C
D (cm)	Sin φ	Sin φ	Sin φ	Sin φ	Sin φ
0.0427	0.1000	0.0940	0.0820	0.0740	0.0620
0.0395	0.1140	0.1080	0.1000	0.0900	0.0740
0.0285	0.1200	0.1120	0.1040	0.0940	0.0780
0.0203	0.1320	0.1260	0.1220	0.1140	0.0960
0.0165	0.1500	0.1400	0.1240	0.1100	0.1020

Table 16: Angle at which rolling occurs with Ethanol As a test liquid at different temperatures.

Θ	30°C	40°C	50°C	60°C	70°C	80°C
D (cm)	Sin φ	Sin φ	Sin φ	Sin φ	Sin φ	Sin φ
0.0427	0.0760	0.0720	0.0660	0.0560	0.0500	0.0440
0.0395	0.0860	0.0800	0.0720	0.0660	0.0600	0.0540
0.0285	0.0800	0.0720	0.0700	0.0660	0.0600	0.0540
0.0203	0.0980	0.0920	0.0860	0.0760	0.0720	0.0640
0.0165	0.1100	0.1060	0.1000	0.0900	0.0860	0.0760
0.0107	0.1560	0.1360	0.1180	0.1100	0.0840	0.0780

Tables 4 -14, show the results of the experiment when the glass spheres of different sizes were tested in both water and Ethanol with temperatures of these matrix liquids increased. The general trend is a decrease in the angle of inclination at which rolling occurs as the temperature increases. The results of Tables 4-9 were summarized in Table 15, and the results of Tables 10 – 14 were summarized in Table 16. The general trend is a decrease in the angle of inclination at which rolling occurs as the temperature increases for each particle size held constant

Table 17: Static friction coefficient μ, intercept A, slope B of the straight line and Hamaker Coefficient A_{132} obtained by calculation for the system studied (water used as a matrix liquid).

T°C	A	B	μ	A_{123}
30	0.0730	2.870×10^{-8}	0.0680	1.986×10^{-15}
40	0.0700	3.151×10^{-8}	0.0560	2.648×10^{-15}
50	0.0670	3.376×10^{-8}	0.0480	3.310×10^{-15}
60	0.0590	3.376×10^{-8}	0.0400	3.972×10^{-15}
70	0.0580	5.154×10^{-8}	0.0525	4.620×10^{-15}
80	0.0510	1.463×10^{-7}	0.1300	5.296×10^{-15}

The data from Tables 17 and 18 show how temperature affects the static friction coefficient (μ), intercept (A), slope (B), and Hamaker coefficient (A_{132}) when using water and ethanol as matrix liquids. In the water-based system, the static friction coefficient starts at 0.0680 at 30°C and increases to 0.1300 by 80°C. This suggests that as the temperature rises, the surfaces experience more friction. The Hamaker coefficient also increases, starting at 1.986×10^{-15} at 30°C and reaching 5.296×10^{-15} at 80°C, meaning that van der Waals forces become stronger at higher temperatures. Similarly, the slope (B) grows from 2.870×10^{-8} to 1.463×10^{-7}, reinforcing this trend.

Table 18: Static friction coefficient μ, intercept A, slope B of the straight line and Hamaker Coefficient A_{132} obtained by calculation for the system studied (Ethanol used as a matrix liquid).

T°C	A	B	μ	A_{132}
30	0.0990	2.307×10^{-8}	0.0480	2.262×10^{-15}
40	0.0940	2.820×10^{-8}	0.0440	3.016×10^{-15}
50	0.0860	3.285×10^{-8}	0.0410	3.770×10^{-15}
60	0.0780	3.480×10^{-8}	0.0362	4.524×10^{-15}
70	0.0620	3.657×10^{-8}	0.0326	5.278×10^{-15}

For the ethanol-based system, the friction coefficient decreases slightly with temperature, from 0.0480 at 30°C to 0.0326 at 70°C. The Hamaker coefficient follows the same increasing pattern as in water, starting at 2.262×10^{-15} and reaching 5.278×10^{-15}. This suggests that while van der Waals forces strengthen with temperature in both cases, ethanol reduces friction more effectively than water. This difference could be useful in applications where lower adhesion is preferred, such as lubrication or surface coatings.

The experiment examined the angles of inclination at which glass spheres rolled in water and ethanol at room temperature. The results indicated that rolling occurred at smaller angles in ethanol than in water, suggesting that lower liquid density reduces adhesion. This finding agreed with [26], who observed that particles in lower-density fluids experience less resistance, leading to earlier movement. In contrast, [27] found that fluid viscosity played a more significant role than density in adhesion strength. Further analysis revealed that rolling angles increased as particle size decreased, demonstrating that apparent weight affects adhesion. This aligns with the findings of [28], who reported that smaller particles exhibit stronger surface interactions due to greater van der Waals forces. In a related study, [29] confirmed that friction coefficients decreased with increasing temperature, supporting the trend observed in the water matrix experiments at different temperatures. The calculation of Hamaker coefficients confirmed weak van der Waals interactions, with values ranging from one point three two times ten to the power of minus fifteen to one point five zero times ten to the power of minus fifteen millijoules per square meter. This validates the assumption that electrostatic effects were negligible.

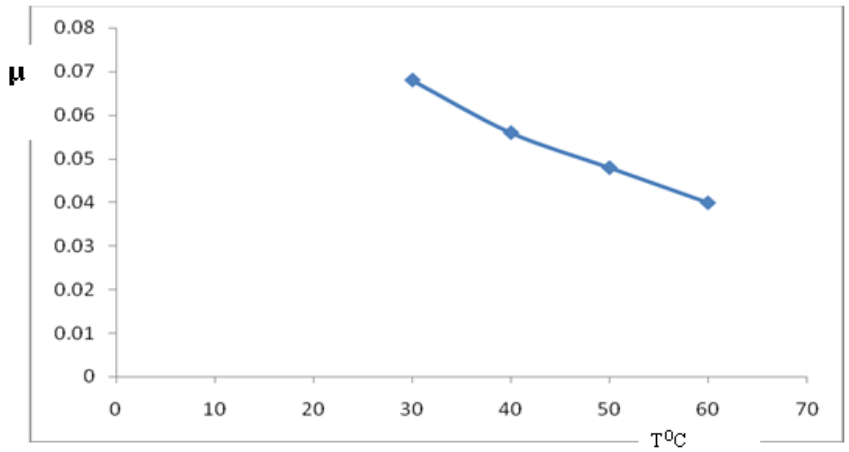


Figure 1: The Effect of Temperature Upon Coefficient of Friction, with Water as a Matrix Liquid.

Figure 1 shows the effect of temperature upon coefficient of friction in water. The coefficient of friction decreased with increasing temperature. This shows that temperature affects friction between a particle and a substrate in a liquid matrix. Increase in temperature reduces friction between the particles and the substrate.

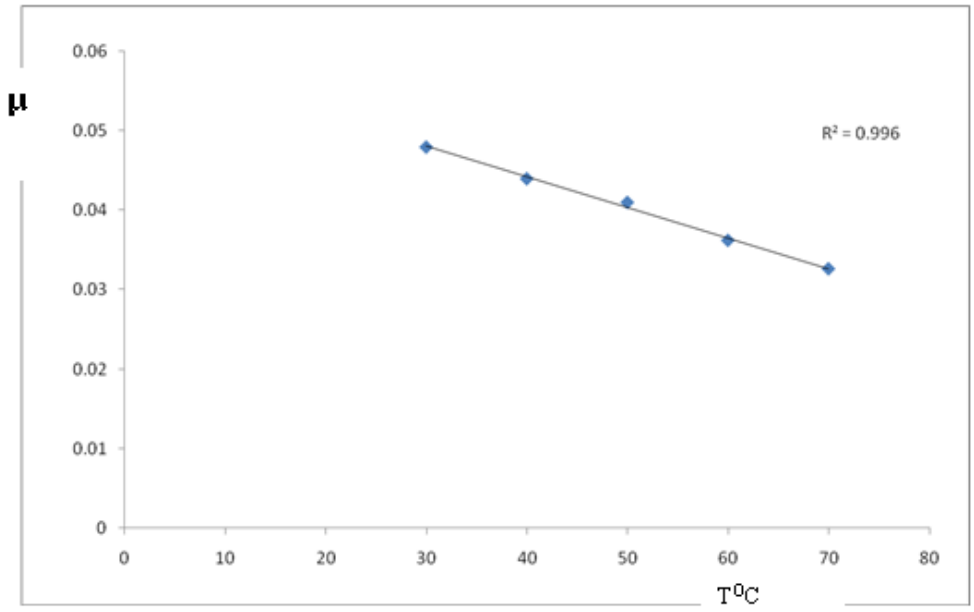


Figure 2: The Effect of Temperature Upon Coefficient of Friction, with Ethanol as a Matrix Liquid.

Figure 2 shows the effect of temperature upon coefficient of friction in Ethanol. The coefficient of friction decreased with increasing temperature. This shows that temperature affects friction between a particle and a substrate in a liquid matrix. Increase in temperature reduces friction between the particles and the substrate. Figure 3 shows the effect of temperature upon Hamaker coefficient in water. The Hamaker coefficient increased with increasing temperature. This gave a positive slope which shows that the Hamaker coefficient is positive. When the Hamaker coefficient is positive, the van der Waals forces are attractive. The value of correlation coefficient obtained shows a relationship between the temperature and Hamaker coefficient.

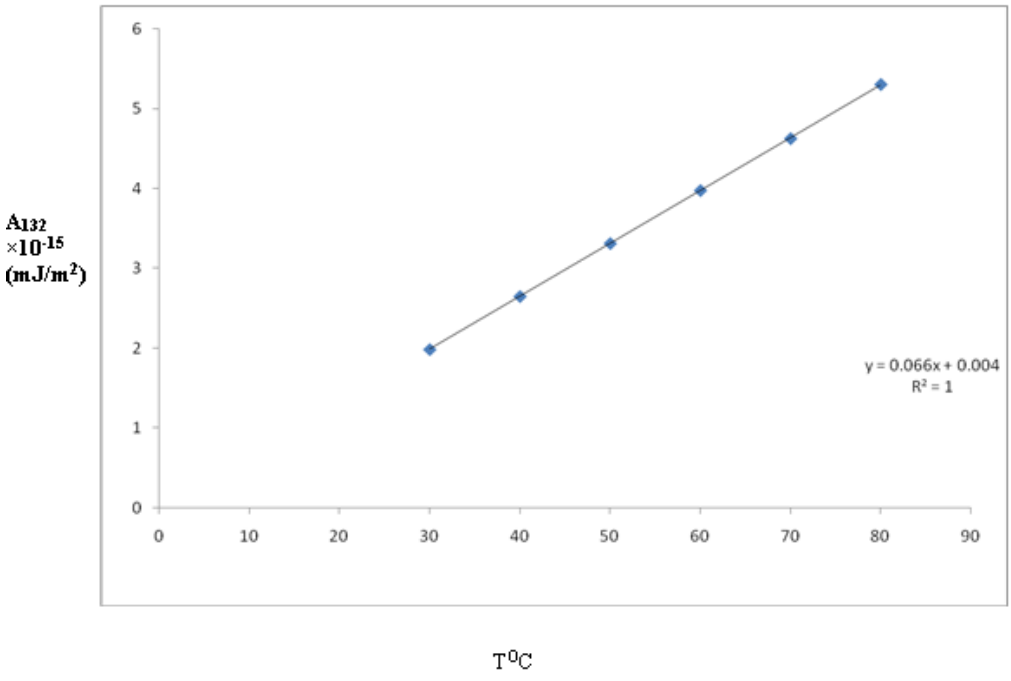


Figure 3: The Effect of Temperature Upon Hamaker Coefficient, with Water as a Matrix Liquid.

Figure 4 shows the effect of temperature upon Hamaker coefficient in Ethanol. The Hamaker coefficient increased with increasing temperature. This gave a positive slope which shows that the Hamaker coefficient is positive. When the Hamaker coefficient is positive, the van der Waals forces are attractive. The value of correlation coefficient obtained shows a relationship between the temperature and Hamaker coefficient. Figure 5 shows the effect of temperature upon the angle of inclination for the particle size of diameter 0.0427cm in water. The angle of inclination decreased as temperature was increased. This shows that

particles sizes affect adhesion in a liquid matrix. Smaller particles will adhere longer to the substrate than the larger particles. Also, the value of the correlation coefficient, shows a relationship between the temperature and the angle of inclination.

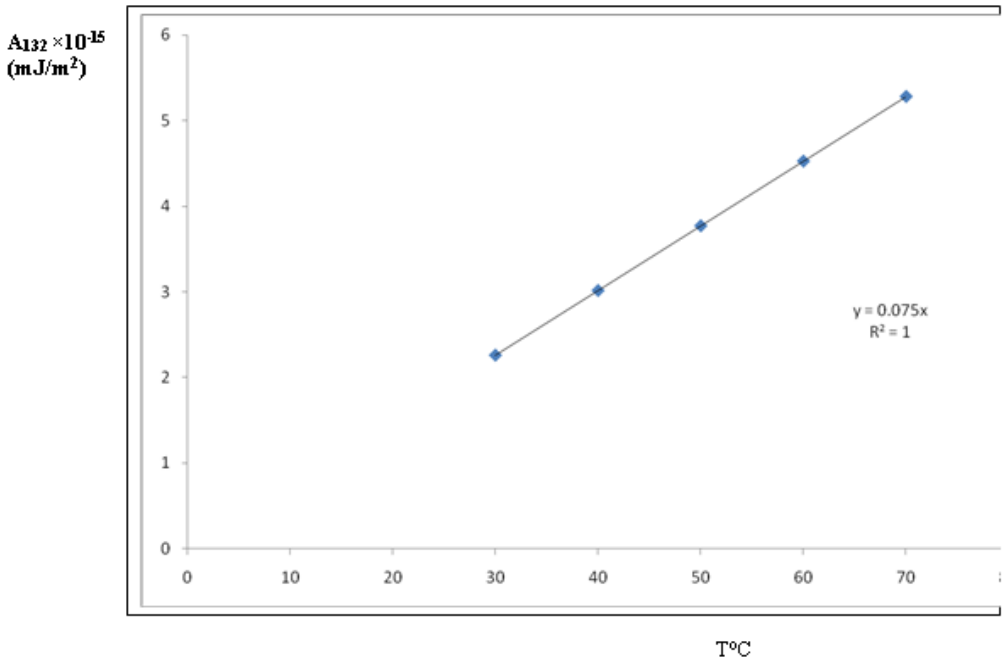


Figure 4 The Effect of Temperature Upon Hamaker Coefficient, with Ethanol as a Matrix Liquid**.**

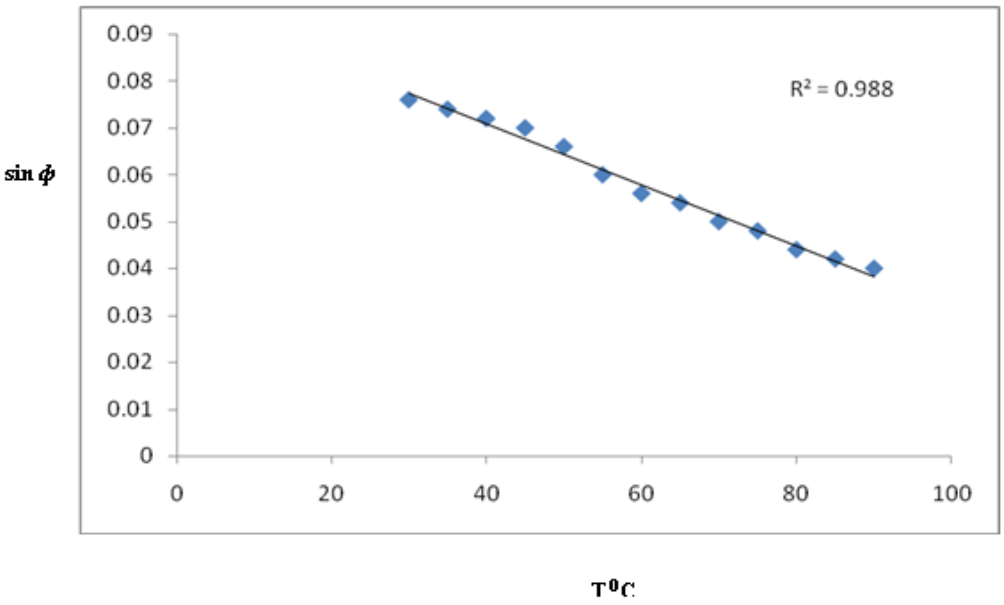


Figure 5: The Effect of Temperature Upon Angle of Inclination for D = 0.0427cm, with Water as A Matrix Liquid.

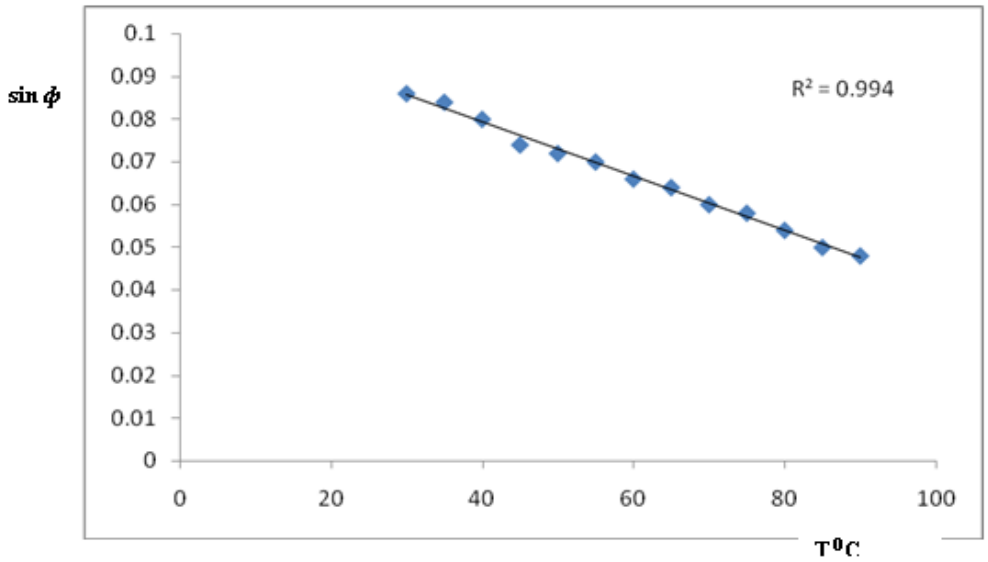


Figure 6: The Effect of Temperature Upon Angle of Inclination for D = 0.0395cm, with Water as A Matrix Liquid.

Figure 6 shows the effect of temperature upon the angle of inclination for the particle size of diameter 0.0395cm in water. The angle of inclination decreased as temperature was increased. This shows that particles sizes affect adhesion in a liquid matrix. Smaller particles will adhere longer to the substrate than the larger particles. Also, the value of the correlation coefficient, shows a relationship between the temperature and the angle of inclination.

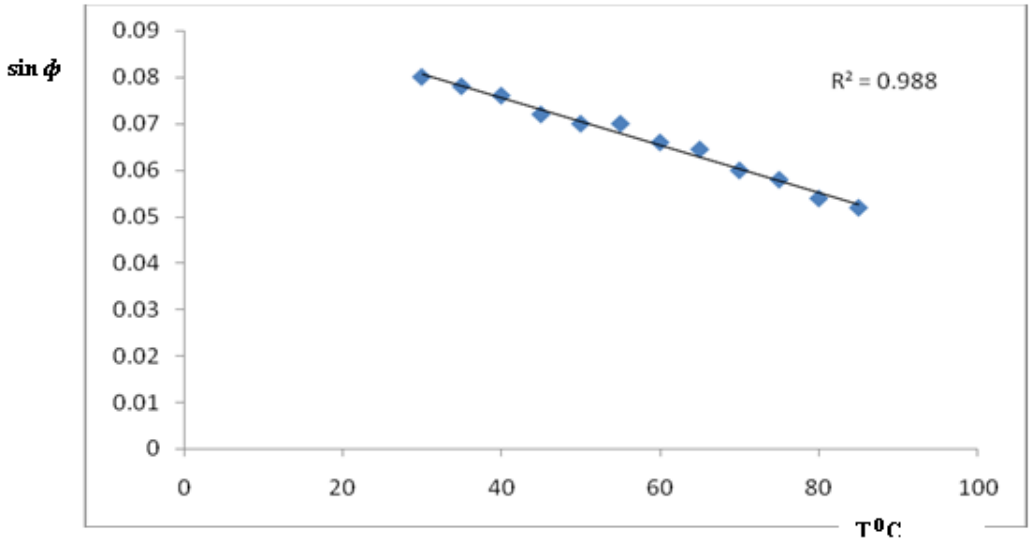


Figure 7: The Effect of Temperature Upon Angle of Inclination for D = 0.0285cm, with Water as a Matrix Liquid.

Figure 7 shows the effect of temperature upon the angle of inclination for the particle size of diameter 0.0285cm in water. The angle of inclination decreased as temperature was increased. This shows that particles sizes affect adhesion in a liquid matrix. Smaller particles will adhere longer to the substrate than the larger particles. Also, the value of the correlation coefficient, shows a relationship between the temperature and the angle of inclination

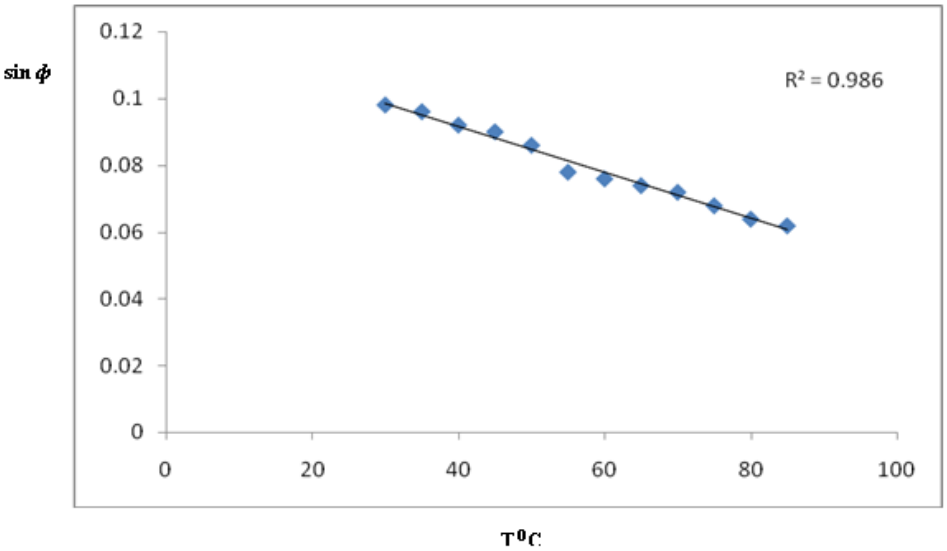


Figure 8: The Effect of Temperature Upon Angle of Inclination for D = 0.0203cm, with Water as a Matrix Liquid.

Figure 8 shows the effect of temperature upon the angle of inclination for the particle size of diameter 0.0203cm in water. The angle of inclination decreased as temperature was increased. This shows that particles sizes affect adhesion in a liquid matrix. Smaller particles will adhere longer to the substrate than the larger particles. Also, the value of the correlation coefficient, shows a relationship between the temperature and the angle of inclination.

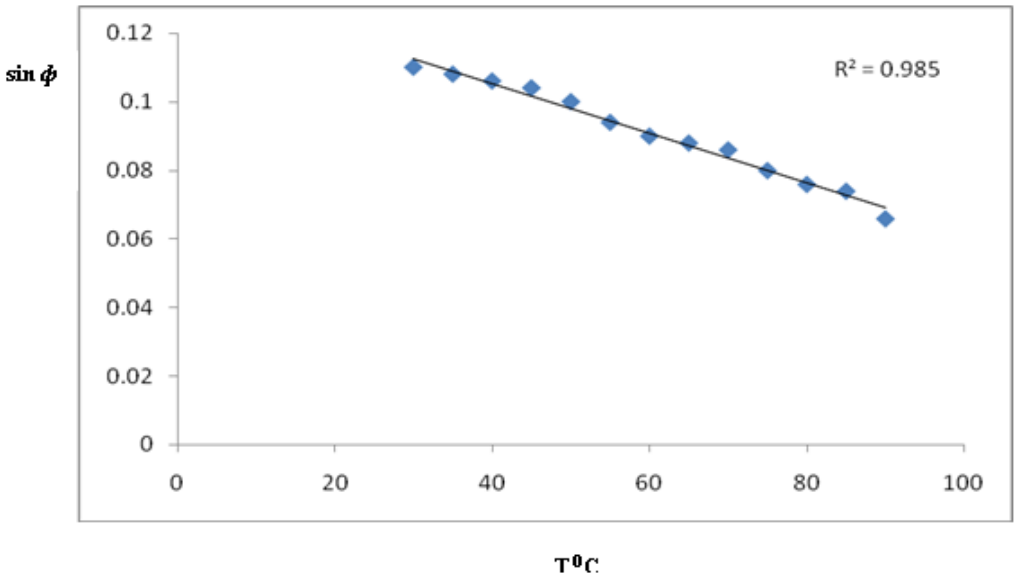


Figure 9 The Effect of Temperature Upon Angle of Inclination for D = 0.0165cm, with Water as a Matrix Liquid.

Figure 9 shows the effect of temperature upon the angle of inclination for the particle size of diameter 0.0165cm in water. The angle of inclination decreased as temperature was increased. This shows that particles sizes affect adhesion in a liquid matrix. Smaller particles will adhere longer to the substrate than the larger particles. Also, the value of the correlation coefficient, shows a relationship between the temperature and the angle of inclination.

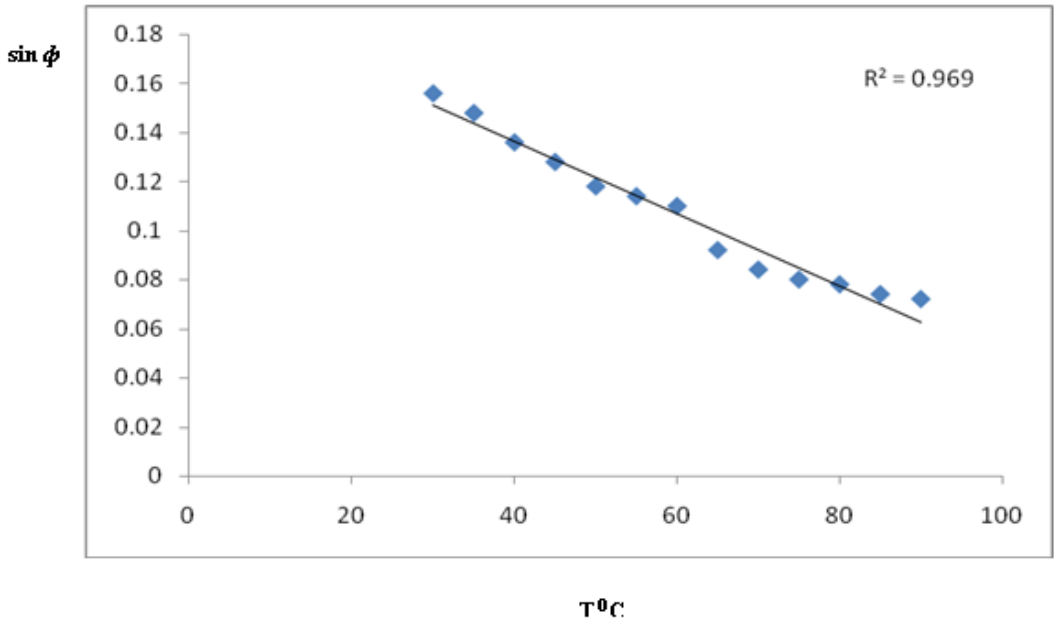


Figure 10, The Effect of Temperature on Angle of Inclination for D = 0.0107cm, with Water as a Matrix Liquid.

Figure 10 shows the effect of temperature upon the angle of inclination for the particle size of diameter 0.0107cm in water. The angle of inclination decreased as temperature was increased. This shows that particles sizes affect adhesion in a liquid matrix. Smaller particles will adhere longer to the substrate than the larger particles. Also, the value of the correlation coefficient, shows a relationship between the temperature and the angle of inclination.

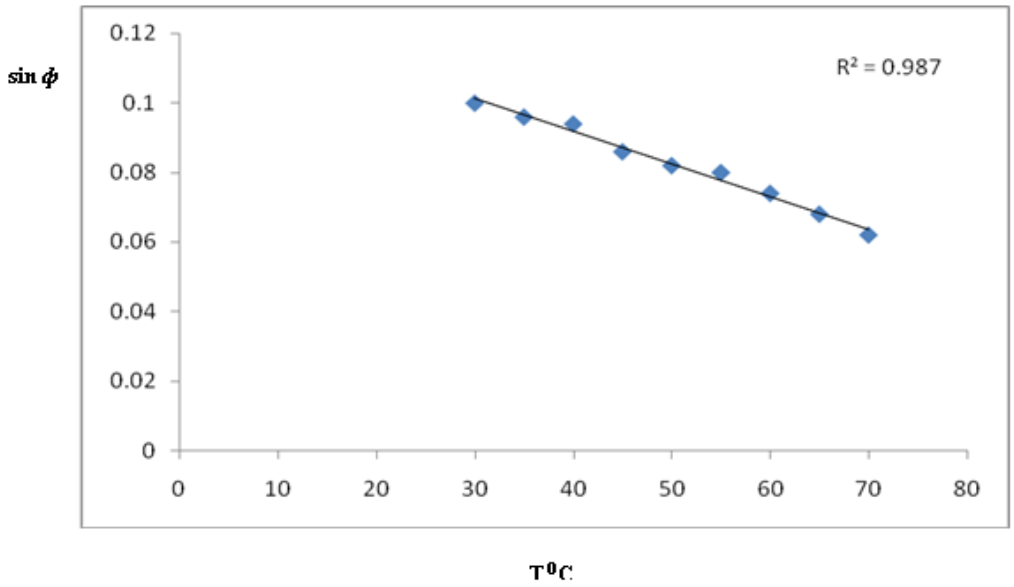


Figure 11 The Effect of Temperature Upon Angle of Inclination for D = 0.0427cm, with Ethanol as a Matrix Liquid.

Figure 11 shows the effect of temperature upon the angle of inclination for the particle size of diameter 0.0427cm in Ethanol. The angle of inclination decreased as temperature was increased. This shows that particles sizes affect adhesion in a liquid matrix. Smaller particles will adhere longer to the substrate than the larger particles. Also, the value of the correlation coefficient, shows a relationship between the temperature and the angle of inclination.

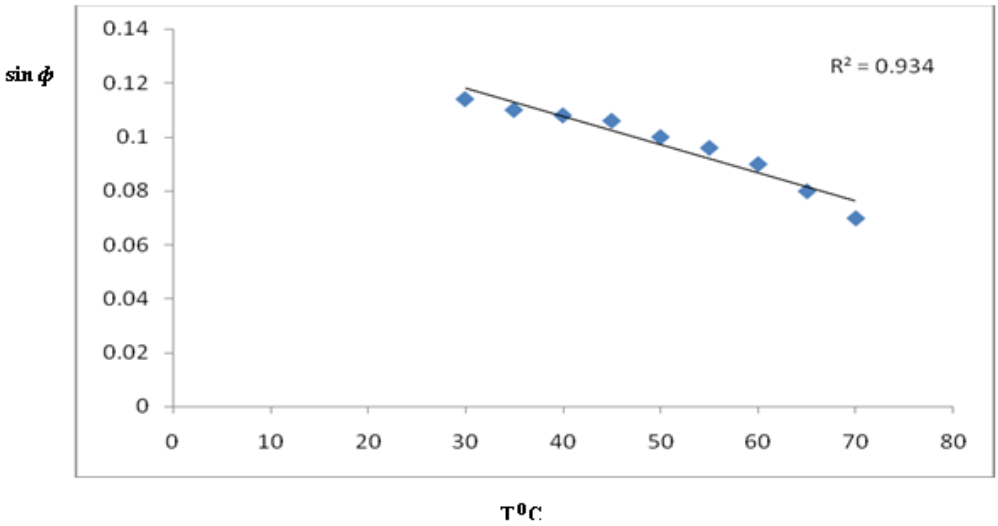


Figure 12: The Effect of Temperature Upon Angle of Inclination for D = 0.0395cm, with Ethanol as a Matrix Liquid**.**

Figure 12 shows the effect of temperature upon the angle of inclination for the particle size of diameter 0.0395cm in Ethanol. The angle of inclination decreased as temperature was increased. This shows that particles sizes affect adhesion in a liquid matrix. Smaller particles will adhere longer to the substrate than the larger particles. Also, the value of the correlation coefficient, shows a relationship between the temperature and the angle of inclination.

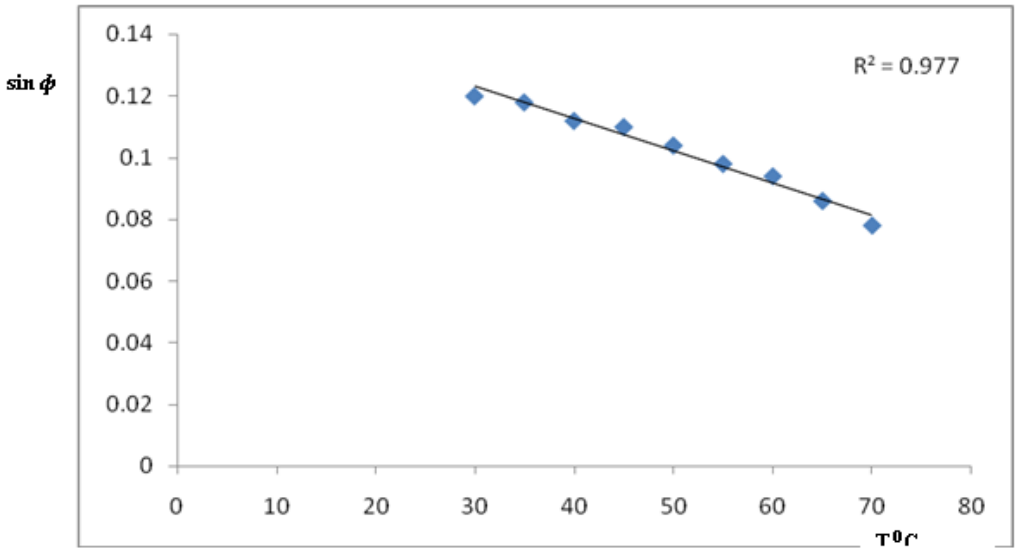


Figure 13: The Effect of Temperature Upon Angle of Inclination for D = 0.0285cm, with Ethanol as a Matrix Liquid**.**

Figure 13 shows the effect of temperature upon the angle of inclination for the particle size of diameter 0.0285cm in Ethanol. The angle of inclination decreased as temperature was increased. This shows that particles sizes affect adhesion in a liquid matrix. Smaller particles will adhere longer to the substrate than the larger particles. Also, the value of the correlation coefficient, shows a relationship between the temperature and the angle of inclination.

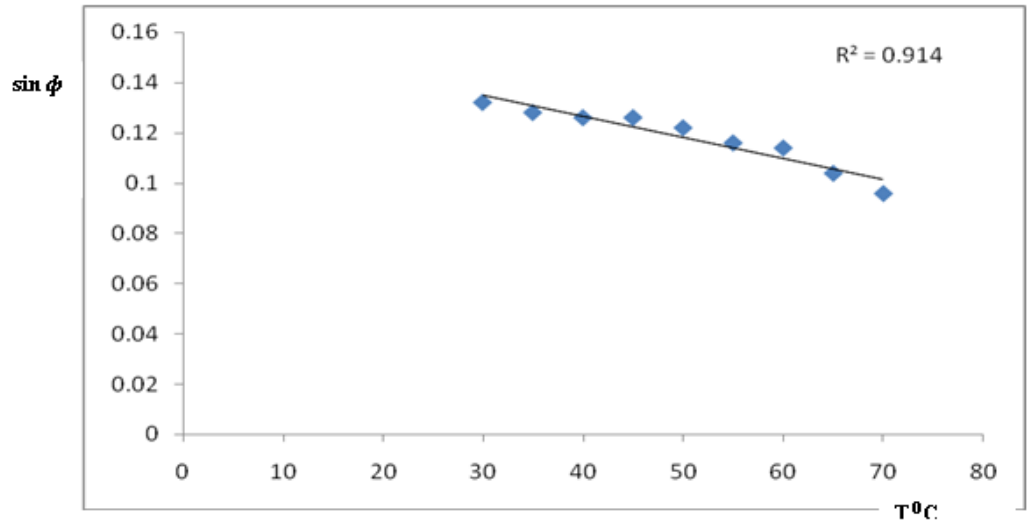


Figure 14: The Effect of Temperature Upon Angle of Inclination for D = 0.0203cm, with Ethanol as a Matrix Liquid.

Figure 14 shows the effect of temperature upon the angle of inclination for the particle size of diameter 0.0203cm in Ethanol. The angle of inclination decreased as temperature was increased. This shows that particles sizes affect adhesion in a liquid matrix. Smaller particles will adhere longer to the substrate than the larger particles. Also, the value of the correlation coefficient, shows a relationship between the temperature and the angle of inclination.

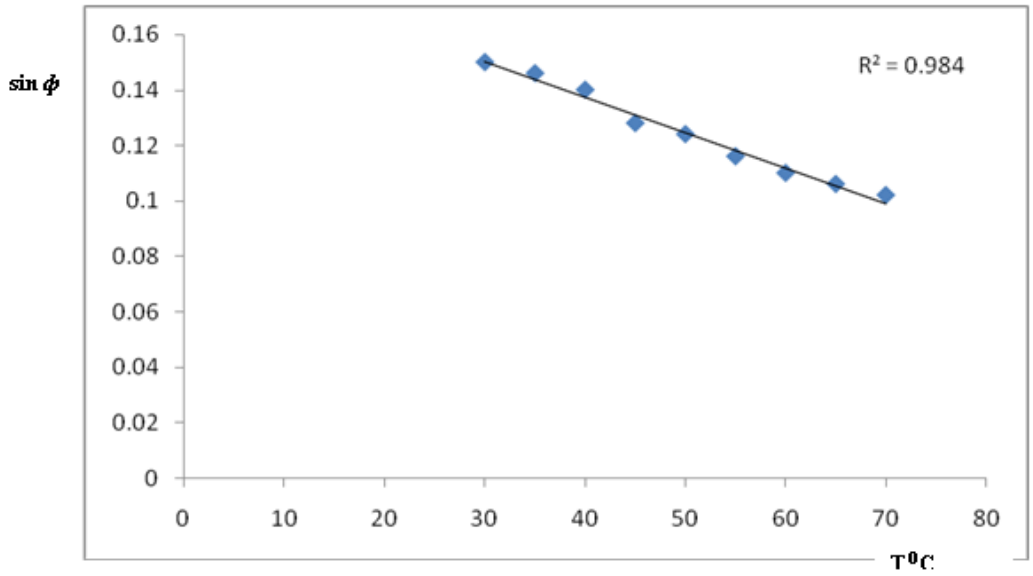


Figure 15: The Effect of Temperature Upon Angle of Inclination for D = 0.0165cm, with Ethanol as a Matrix Liquid.

Figure 15 shows the effect of temperature upon the angle of inclination for the particle size of diameter 0.0165cm in Ethanol. The angle of inclination decreased as temperature was increased. This shows that particles sizes affect adhesion in a liquid matrix. Smaller particles will adhere longer to the substrate than the larger particles. Also, the value of the correlation coefficient, shows a relationship between the temperature and the angle of inclination.

4. Conclusions

The angle of inclination at ambient temperature, increased when the particles sizes were decreased as shown in Tables 1 and 2. But, when the temperature was increased, the angle of inclination decreased for each particle size in both liquids as shown in Tables 4 - 16. This shows that particles sizes affect adhesion. Smaller particles will adhere longer to the substrate than larger particles. The coefficient of friction decreased with increasing temperature as shown in Tables 17 and 18 which were plotted in Figures 3 and 4. This shows that temperature affects friction between a particle and a substrate in a liquid matrix. Hence, increase in temperature reduces friction between the particle and the substrate. At room temperature, the Hamaker coefficient of the two systems studied are between (10^{-14} mJ/m^2 and 10^{-15} mJ/m^2) as shown in Table 3. This would show a weak interaction in the interface. When the temperature was increased, the Hamaker coefficient increased also as shown in Tables 17 and 18. This gave a positive slope when the graph of A_{132} vs T was plotted as shown in Figures 5 and 6. When the Hamaker coefficient is positive,

the van der Waals forces are attractive, but when it is negative, the force is repulsive. Since the values are positive therefore, the van der Waals forces are attractive.

But the increase. Surface tension affects cohesion-force which exists between like particles of the same nature and adhesion which exists between particles of different objects. In case of glass spheres and the substrate, it was observed that at room temperature, the $\sin\phi$ values increased as the sizes of the glass spheres were decreased. But when heat was introduced, $\sin\phi$ values decreased with increase in temperature. It is therefore imperative to note that most liquids increase in volume as their temperatures rise from 0°C and so their densities diminish continuously, water and ethanol are no exceptions. When these liquids are heated, their densities decrease their volumes increase and their masses remain constant. The decrease in the angle of inclination in Ethanol, is due to the decrease in density as a result of increase in temperature, and the nearness to its boiling point. This means that the desired temperatures are quickly attained in ethanol than in water, which has a higher boiling point. The introduction of heat however, reduces the density of liquid at every interval of increment. This lowers the surface tension of the liquid by breaking the weak intermolecular van der Waals forces binding the molecules of the liquids. When this happens, it enhances the faster sliding the particles off from substrate. When the graph of Hamaker coefficient is plotted against temperature in both water and Ethanol, it gave a positive graph, and when the graph is positive, it shows that the Hamaker coefficient is positive. When the Hamaker coefficient is positive, the van der Waals forces will be attractive but these forces are weakened by increased temperature.

Hence, the particles will slip off from the marked point faster thereby lowering the height h of the inclined pane. When heat was not introduced in the experiment, it was also observed that the size of the particle played a major role, as the larger, the particle the quicker it rolls off the plane. The sliding of these particles actually commenced when the angle of inclination was equal to angle of repose. With the introduction of heat to the system, the angle of repose was obtained faster which enabled quicker sliding of the particles. Moreover, critical observation and deductions from Tables 17 and 18 in the calculation of Hamaker Coefficient, show that the variation of coefficients of friction caused by the application of heat which led to temperature variation in Hamaker coefficients as calculated, shows that heat or temperature variation has a tremendous effect on the weak van der Waals force.

Finally, in water, experimental values with large particles were plotted in Figures 1 and 2, and the coefficient of friction and the slope were determined showing significant measurement. But for small particles, the large values of $1/R^2$ cm^{-2} give scattered points which may be due to their irregularities in shape of the glass spheres. Hamaker Coefficients were between 1.320×10^{-15} and 1.508×10^{-15} mJ/m^2, at room temperature as shown in Table 5.3. When the heat was introduced in water, the values of Hamaker Coefficient were between 1.986×10^{-15} and 5.296×10^{-15} mJ/m^2, and for Ethanol, values of Hamaker Coeffient were between 1.320×10^{-15} and 1.320×10^{-15} mJ/m^2, as shown in Tables 17 and 18. They fall in the range of usual values for Hamaker Coefficients (between 10^{-13} and 10^{-15} mJ/m^2 and correspond to rather weak interfacial interactions). This, however, shows that there is weak van der Waals forces responsible for the adhesion of these small particles (glass spheres) suspended in a liquid matrix. And these van der Waals forces are attractive since the Hamaker Coefficient of the systems studied are positive. It is to be noted that for a system with negative Hamaker Coefficient, one would expect a straight line of negative slope in the representation. The graph of $\sin\phi = f(\frac{1}{R^2})$, would cut the horizontal axis for a value $1/R_o^{\,2}$. Glass spheres of radius smaller than R_o (the smallest radius of a spherical glass by which adhesion to a substrate can take place), would not adhere to the substrate but roll off under the slightest external force. For such situations, the distance of separation d from the substrate would be greater than d_o. The value of d would be that giving a repulsive van der Waals force equal to the apparent weight of the particle.

From the experimental results, computations and analysis, the effect of temperature on the sliding of a glass sphere on a substrate immersed in a liquid is to cause the attainment of the angle of repose (angle at which sliding tends to start/begin) to occur at lower angles as temperature increases. It is therefore recommended that students who will walk on this path should take note of the precautions. Also, subsequent research should be done on varying the density of the fluid on adhesion at the onset of sliding. The density may be varied and electrostatic effects may be introduced with common salt (NaCl) at measured values in grammes in liquids like water and Ethanol, or in other covalent liquid like kerosene. It is expected people who will take interest on this, should improve on this great research work and investigate possible factors stated above.

References

[1] Isrealachvili, J., and Tabor, D. Van der Waals Forces: Theory and Experiment. *Progress in Surface and Membrane Science*, 1973. *7*, 1-55.

[2] Hermann, J. DiStasio Jr, R. A, Tkatchenko A. Firstt-Principles Models for van der Waals Interactions in Molecules and Materials: Concepts, Theory, and Applications, Chem. Rev. 2017. 117, 6, 4714–4758.

[3] Feng, J. Q., & Hays, D. A. Relative importance of electrostatic forces on powder particles. *Powder Technology*, 2003. *135*, 65-75

[4] Lefèvre, C., Bouadjar, B., Ferrand, V., Tadini, G., Mégarbané, A., Lathrop, M., Prud'homme, J.F. and Fischer, J. Mutations in a new cytochrome P450 gene in lamellar ichthyosis type 3. *Human Molecular Genetics*, 2006. *15*(5), pp.767-776.

[5] Burger, F. A., John, J. G., and Frölicher, T. L. Increase in ocean acidity variability and extremes under increasing atmospheric CO 2. *Biogeosciences*, 2020. *17*(18), 4633-4662.

[6] Gaddam, P., & Ducker, W. Electrostatic screening length in concentrated salt solutions. *Langmuir*, 2019. *35*(17), 5719-5727.

[7] Hamaker, H. C. The London—van der Waals attraction between spherical particles. *physica*, 1937. *4*(10), 1058-1072.
[8] Tadros, T. F. (Ed.). *Colloids in paints*. John Wiley & Sons, 2011.
[9] Smith, D. K. W., & Kitchener, J. A. The strength of aggregates formed in flocculation. *Chemical Engineering Science*, 1978. *33*(12), 1631-1636.
[10] Ulusoy, U. A Review of Particle Shape Effects on Material Properties for Various Engineering Applications: From Macro to Nanoscale. *Minerals*, 2023. *13*, 91.
[11] Goldman, A. J. Cox, R. G, Brenner, H. Slow viscous motion of a sphere parallel to a plane surface. The Physics of Fluids, 1967. vol. 10, pages 637-650.
[12] Fillingham, P., Kottapalli, K., Zhan, X., and Novosselov, I. V. Characterization of adhesion force in aerodynamic particle resuspension. *Journal of aerosol science*, 2019. *128*, 89-98.
[13] Marques, A.C.; Mocanu, A.; Tomić, N.Z.; Balos, S.; Stammen, E.; Lundevall, A.; Abrahami, S.T.; Günther, R.; de Kok, J.M.M.; Teixeira de Freitas, S. Review on Adhesives and Surface Treatments for Structural Applications: Recent Developments on Sustainability and Implementation for Metal and Composite Substrates. *Materials*, 2020. *13*, 5590.
[14] Corn, M and Stein, F. ***In Aerosol Science***, C.N Davis, Ed, (Academic Press, London, 1966. pp. 359-392.
[15] Krupp, H. Particle adhesion theory and experiment. *Advan. Colloid Interface Sci.*, 1967. *1*, 111-239.
[16] Shrestha, N., Shad, M. Y., Ulvi, O., Khan, M. H., Karamehic-Muratovic, A., Nguyen, U.S.D., Baghbanzadeh, M., Wardrup, R., Aghamohammadi, N., Cervantes, D. and Nahiduzzaman, K.M. The impact of COVID-19 on globalization. *One Health*, 2020. p.100180.
[17] Wettlaufer J. S. and M. Worster G. Premelting dynamics, *Annual Review of Fluid mechanics, 2006.* Vol. 38:427-452.
[18] Van-Oss, C.J., Omenyi, S.N. and Newmann, A.W. *Coiloid Polymer Sci.* 1979. 257,737.
[19] Omenyi, S.N. and Newmann, A.W.J. *Appl. Phys*. 1976. 47, 3956.
[20] Omenyi, S.N. Smith, R.P and Newmann, A.W.J. *Colloid Interface Sci*. 1980. 75,117.
[21] Salahshoori I., Jorabchi, M. N., Mazaheri, A., Mirnezami, S. M. S., Afshar, M, Golriz, M., Marcos A.L. Nobre, M. A. L. Tackling antibiotic contaminations in wastewater with novel Modified-MOF nanostructures: A study of molecular simulations and DFT calculations. Environmental Research, 2024. vol. 252, Part 2, 118856
[22] Owe Berg, T. G. Background Spectra of Solids. *Journal of the Optical Society of America*, 1961. *51*(6), 697-698.
[23] Paajanen, M, Katainen, J, Pakarinen, O. H, Foster, A. S, Lahtinen, J. Experimental humidity dependency of small particle adhesion on silica and titania, Journal of Colloid and Interface Science, 2006. 304 (2006) 518-523
[24] Beaudoin, S., Jaiswal, R., & Kilroy, C. Particle and Thin Film Adhesion, 2007.
[25] Katre, A., Bertossi, T., Clarke-Sather, A., & Parsatoon, M. Agroecological transition: A territorial examination of the simultaneity of limited farmer livelihoods and food insecurity. *Sustainability*, 2022. *14*(6), 3160.
[26] Meng, Y., Deng, J., Wu, J., Wang, R., & Lu, Y. Improved interfacial adhesion of AlTiN coating by micro-grooves using ultrasonic surface rolling processing. *Journal of Materials Processing Technology*, 2022. *304*, 117570.
[27] Ghasaban, S., Imani, M., & Atai, M. Correlation between composition and adhesion properties of a zinc oxide-filled, acrylate pressure sensitive adhesive: An experimental design approach. *International Journal of Adhesion and Adhesives*, 2023. *127*, 103528.
[28] Sato, N., Aoyama, Y., Yamanaka, J., Toyotama, A., & Okuzono, T. Particle adsorption on hydrogel surfaces in aqueous media due to van der Waals attraction. *Scientific reports*, 2017. *7*(1), 6099.
[29] Mhamdi Alaoui, H., Zhao, C., Niu, W., & Yang, Z. Investigating temperature effects on the shear behavior of clays: Molecular dynamics simulations. *Canadian Geotechnical Journal*, 2024. *62*, 1-23.